

# Three- and four-body interactions in colloidal systems

Jure Dobnikar

*University of Graz, Institute for Chemistry, Heinrichstrasse 28, 8010 Graz, Austria  
Institute Jožef Stefan, Jamova 39, 1000 Ljubljana, Slovenia\**

Matthias Brunner, Jörg Baumgartl, and Clemens Bechinger

*University of Stuttgart, 2. Physikalisches Institut, 70550 Stuttgart, Germany*

Hans-Hennig von Grünberg

*University of Graz, Institute for Chemistry, Heinrichstrasse 28, 8010 Graz, Austria*

(Dated: May 6, 2019)

Three-body and four-body interactions have been directly measured in a colloidal system comprised of three (or four) charged colloidal particles. Two of the particles have been confined by means of a scanned laser tweezers to a line-shaped optical trap where they diffused due to thermal fluctuations. By means of an additional focused optical trap a third particle has been approached and attractive three-body interactions have been observed. These observations are in qualitative agreement with additionally performed nonlinear Poisson-Boltzmann calculations. Two configurations of four particles have been studied experimentally as well and in both cases a repulsive four-body interaction term has been observed.

PACS numbers: Valid PACS appear here

## I. INTRODUCTION

The total interaction energy of a system comprised of  $N$  particles consists of pair terms, three-body, four-body, ... and  $N$ -body contributions. The complete description of such a system should, in principle, take into account all these terms. In practice, however, the  $N$ -body terms are rarely known, and even if they are, it is a formidable task to include even a few lower order terms in any physical theory. So, in most cases, the description is grossly simplified by approximating the complete many-body description of the system by *effective* pair interactions. All higher many-body terms are integrated out into the effective parameters appearing in the effective pair interactions. Due to the pairwise additivity of the simplified model, the evaluation of physical properties of the system becomes tractable, but one should be aware of the following limitations.

The effective pair interactions are highly integrated quantities and depend on the particular many-body configuration of the system. Therefore, there is no unique effective pair interaction describing a system. Moreover, the simplification very often leads to thermodynamic inconsistencies [1]. The effective quantities depend on the state of the system, i.e. density, and even on the arrangement of the particles in space. This is illustrated in [2, 3, 5] where the effective pair interactions are determined in a solution of charged colloids. In [5] the effective interactions are extracted from radial distribution functions measured in a 2D colloidal suspension at different densities. In those experiments a clear dependence of the results on the density of colloids has been observed. In [2, 3, 4] the effective pair interactions have been studied numerically in a 3D colloidal suspension, solving the non-linear Poisson-Boltzmann equation and integrating out the many-body terms. The resulting effective pair interaction was different when the colloids were placed in a FCC lattice than when they were forming a BCC lattice.

These examples illustrate that the effective potentials extracted from experimental studies by simply determining the effective parameters to achieve agreement between theory and experiment may well work, but as we have seen, it is not a fundamental approach and has severe limits of applicability. Any correct physical description of a many-body system should therefore take many-body terms into account.

Already in 1943 it has been supposed by Axilrod and Teller (AT) [6] and later also by Barker and Henderson [7] that three-body interactions may significantly contribute to the total interaction energy in noble gas systems. This seems to be surprising because noble gas atoms possess a closed-shell electronic structure and are therefore often (and erroneously) regarded as an example of a simple liquid. The conjecture of Axilrod and Teller, however, was confirmed only very recently, when large-scale molecular dynamics simulations for liquid xenon and krypton [8, 9] was compared

---

\*Electronic address: jure.dobnikar@uni-graz.at

with structure factor measurements at small q-vectors performed with small-angle neutron scattering [10, 11]. In these papers it has clearly been demonstrated that only a combination of pair-potentials and three-body interactions, the latter in the form of the AT-triple-dipole term [6], leads to a satisfactory agreement with the experimental data. In the meantime, it has been realized that many-body interactions have to be considered also for nuclear interactions [12], inter atomic potentials, electron screening in metals [13], photo-ionization, island distribution on surfaces [14], and even for the simplest chemical processes in solids [15] like breaking or making of a bond.

In view of the general importance of many-body effects it seems surprising that until now no direct measurements of these interactions have been performed. This is largely due to the fact that in atomic systems, positional information is typically provided by structure factors or pair-correlation functions, i.e. in an integrated form. Direct measurements of many-body interactions, however, require direct positional information beyond the level of pair-correlations, which is not accessible in atomic or nuclear systems. In contrast to that, owing to the convenient time and length scales involved, the microscopic information is directly accessible in colloidal suspensions. In addition, the pair-interactions in colloidal suspensions can be varied over large ranges, e.g. from short-ranged steric to long-ranged electrostatic or even dipole-dipole interactions.

In the present study [17, 18] we used charged colloidal particles whose interactions are mediated by the microscopic ions in the electrolyte. The pair interaction in such systems is directly related to the overlap of the ion clouds (double-layers) which form around the individual colloids and whose thickness is determined by the ionic strength of the solution. In highly de-ionized solutions, these double-layers can extend over considerable distances. If more than two colloids are within the range of such an extended double layer, many-body interactions are inevitably the consequence. Accordingly, deviations from pair-wise additive interactions are expected under low salt conditions and high densities of colloids.

Experimental evidence for many-body interactions has been already obtained from effective pair-interaction potential measurements of two-dimensional (2D) colloidal systems. Upon variation of the particle density, a characteristic dependence of the effective pair interaction was found which has been interpreted in terms of many-body interactions [5]. However, during those studies the relative contributions of different many-body terms could not be further resolved. Performing the experiment described in this paper, i.e. observing the system of only three (or four) particles, we were able to measure the three- and four-body interactions directly.

## II. EXPERIMENTAL SYSTEM

As colloidal particles we used charge-stabilized silica spheres with 990nm diameter suspended in water. A highly diluted suspension was confined in a silica glass cuvette with  $200\mu\text{m}$  spacing. The cuvette was connected to a closed circuit, to deionize the suspension and thus to increase the interaction range between the spheres. This circuit consisted of the sample cell, an electrical conductivity meter, a vessel of ion exchange resin, a reservoir basin and a peristaltic pump [19]. Before each measurement the water was pumped through the ion exchanger and typical ionic conductivities below  $0.07\mu\text{S}/\text{cm}$  were obtained. Afterwards a highly diluted colloidal suspension was injected into the cell, which was then disconnected from the circuit during the measurements. This procedure yielded stable and reproducible ionic conditions during the experiments. Due to the ion diffusion into the sample cell, the screening length  $\kappa^{-1}$  decreased linearly with time during the measurements. The rate of change of the screening length, however, was only less than half a percent per hour, which means that in the time needed to perform a complete set of measurements, the ionic concentration did not change more than about 1 percent. This tiny variation has been taken into account when performing the PB calculations (see section IV.).

After the particles sedimented down to the bottom plate of the sample cell, they were brought in the field of view of the microscope (Fig.1). Two particles were trapped with line-scanned optical tweezers, which was created by the beam of an argon ion laser being deflected by a computer-controlled galvanostatically driven mirror with a frequency of approximately 350Hz. The time averaged intensity along the scanned line was chosen to be Gaussian-distributed with the half-width  $\sigma_x \approx 4.5 \mu\text{m}$ . The laser intensity distribution perpendicular to the trap was given by the spot size of the laser focus, which is also Gaussian with  $\sigma_y \approx 0.5 \mu\text{m}$ . This yielded an external laser potential acting as a stable quasistatic trap for the particles. Due to the negatively charged silica substrate, the particles also experience a repulsive vertical force, which is balanced by the particle weight and the vertical component of the light force. Due to the fact that the potential is much steeper in the vertical direction than the in the  $xy$  plane, the vertical particle fluctuations can be disregarded. The particles were imaged with a long-distance, high numerical aperture microscope objective (magnification  $\times 63$ ) onto a CCD camera and the images were stored every 120 ms. The lateral positions of the particle centers were determined with a resolution of about 25 nm by a particle recognition algorithm.

Three- and four-body interaction potentials were measured in this setup by performing the following steps (which will be explained in detail below): First only one particle was inserted into the trap and its position probability

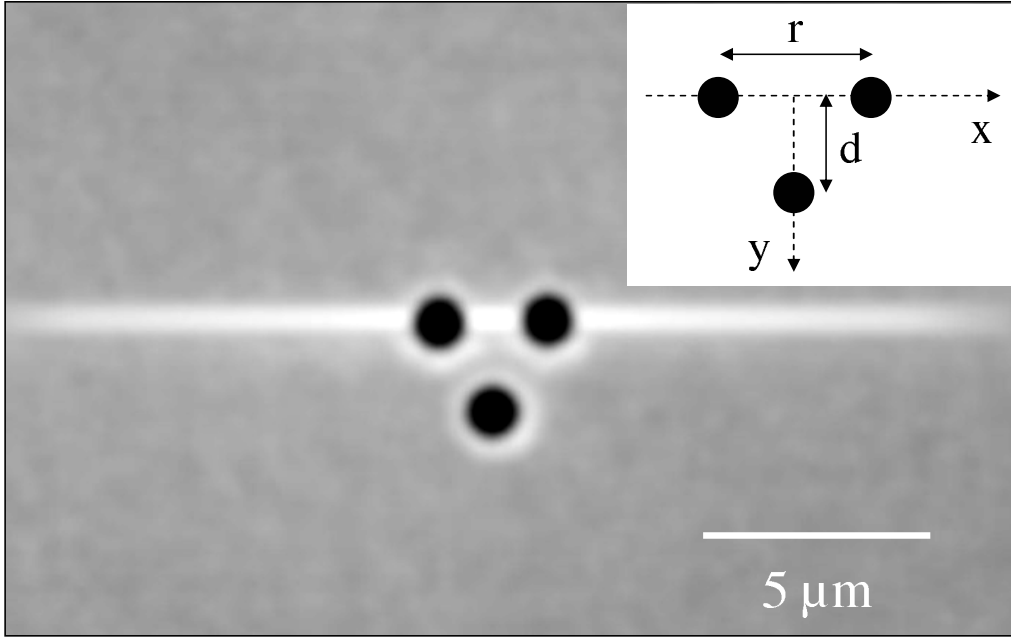


FIG. 1: Photograph of sample cell with two silica particles confined to a light trap created by an optical tweezers and a third particle trapped in a focused laser beam. The inset shows a schematic drawing of the experimental geometry.

distribution was evaluated from the recorded positions. From this the external laser potential  $u_L$  could be extracted. Next, we inserted two particles in the trap and measured their distance distribution. From this, the pair-interaction potential was obtained. Finally, a third particle was made to approach to the optical trap by means of additional point optical tweezers (focus size  $\approx 1.3 \mu\text{m}$ ), which held this particle at a fixed position during the measurement. From the distance distribution of the first two particles we obtained the total interaction potential for the three particles. Finally, we subtracted a superposition of pair potentials (known from the previous two-particle measurements) from the total interaction energy to obtain the three-body interaction. The same procedure was done with four particles to determine the four-body interaction. The fourth particle was fixed with additional point laser tweezers. The many-body term obtained after subtracting the pair terms was now the sum of three- and four-body interactions.

### III. DATA EVALUATION AND EXPERIMENTAL RESULTS

We first determined the external potential acting on a single particle due to the optical line trap. The probability distribution  $P(x, y)$  of finding a particle at the position  $(x, y)$  in the trap was evaluated from the recorded positions.  $P(x, y)$  depends only on the temperature and the external potential  $u_L(x, y)$  created by the laser tweezers. According to the Boltzmann probability distribution  $P(x, y) = P_L e^{-\beta u_L(x, y)}$ , with  $P_L$  being a normalization constant. Taking the logarithm of  $P(x, y)$  yields the external potential  $u_L(x, y)$  with an offset given by  $\log P_L$ . The probability distributions in  $x$  and  $y$  directions are statistically independent, and can therefore be factorized. The laser potential is thus  $u_L(x, y) = u_L(x) + u_L(y)$ . The potential along the  $x$  axis is shown in Fig.2 for various laser intensities. As can be seen, all renormalized potentials fall, within our experimental resolution, on top of each other. This clearly demonstrates that the optical forces exerted on the particles scale linearly with the input laser intensity. This fact allows us to use different external laser powers for two-, three- and four-body experiments (in the three- and four-body experiment, due to the additional repulsion of the third particle, a stronger laser power is needed to keep the mean distance between the two particles similar). The corresponding potential in the perpendicular ( $y$ ) direction has the same (Gaussian) shape, but it is much steeper due to the chosen scanning direction. Therefore, the particles hardly move in the  $y$  direction during a measurement.

Next, we inserted a second particle in the trap. The four-dimensional probability distribution is now  $P(x_1, y_1, x_2, y_2) = P_{12} e^{-\beta(u_L(x_1, y_1) + u_L(x_2, y_2) + U(r))}$ , with  $x_i$  and  $y_i$  being the positions of the  $i$ -th particle relative to the laser potential minimum and  $U(r)$  the distance dependent pair-interaction potential between the particles. This can be projected to

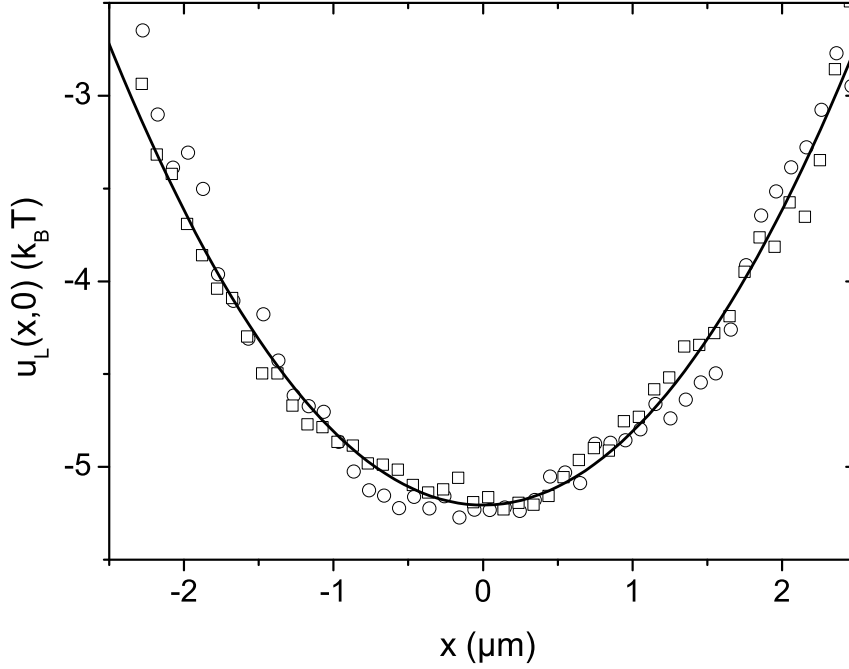


FIG. 2: The shape of the laser potential along the tweezers line for three different laser intensities (symbols: triangles 100mW, circles 200mW and squares 500mW); for better comparison all curves are normalized to an intensity of 100mW. The Gaussian fit is plotted as a solid line.

$$\begin{aligned}
 P(r) &= \iiint\iiint P(x_1, y_1, x_2, y_2) \delta\left(\sqrt{(x_1 - x_2)^2 + (y_1 - y_2)^2} - r\right) dx_1 dx_2 dy_1 dy_2 = \\
 &= P_{12} e^{-\beta U(r)} \iiint\iiint e^{-\beta(u_L(x_1, y_1) + u_L(x_2, y_2))} \delta\left(\sqrt{(x_1 - x_2)^2 + (y_1 - y_2)^2} - r\right) dx_1 dx_2 dy_1 dy_2 \quad (1)
 \end{aligned}$$

In principle the integral is constituted of all possible configurations of two particles with distance  $r$ . Performing the full four-dimensional integration, however, is difficult because of the limited experimental statistics. This problem can be overcome by the following two considerations. First, due to the Gaussian shape of the external potential, the most likely particle configurations are symmetric with respect to the potential minimum of  $u_L$  (any asymmetric configuration for constant  $r$  has a higher energy). Secondly, particle displacements in  $y$ -direction are energetically unfavorable because  $\sigma_x \gg \sigma_y$ . Accordingly, for  $r = \text{const}$  the minimum energy configuration is  $(x_1 = r/2, y_1 = 0, x_2 = -r/2, y_2 = 0)$ . It has been confirmed by a simple calculation with the experimental parameters that all other configurations account for only for less than 1 percent of the value of the integral in Eq.(1). Accordingly, Eq.(1) reduces to

$$P(r) = P_0 e^{-\beta(U(r) + 2u_L(r/2, 0))} . \quad (2)$$

Since  $u_L(x, y)$  is known from the previous one-colloid measurement, we can obtain the interaction potential  $U(r)$  from the measured  $P(r)$ ,

$$\beta U(r) = -\log P(r) - 2\beta u_L(r/2, 0) + \log P_0 . \quad (3)$$

The normalization constant  $P_0$  was chosen in a way that  $U(r) \rightarrow 0$  for large particle separations  $r$ . We first measured  $U(r)$  according to the above procedure in the absence of a third particle. As expected, the negatively charged colloids experience a strong electrostatic repulsion which increases with decreasing distance. The pair-interaction potential of

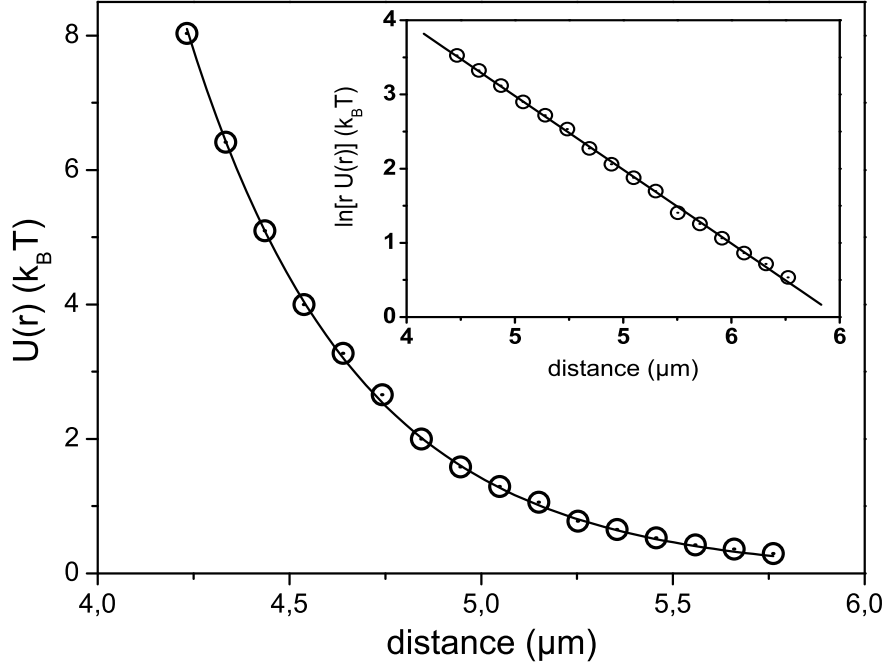


FIG. 3: Measured pair-interaction potentials  $U(r) = u_{pair}(r)$  (symbols) in the absence of the third particle. The data agree well with a DLVO potential, Eq.(4) (solid line). In the inset the potential is multiplied by  $r$  and plotted logarithmically, so that the DLVO expression, Eq.(4) transforms into a straight line. From a fit we obtained the effective charge  $Z^* \approx 6500$  and the screening length  $\kappa^{-1} \approx 470\text{nm}$ .

two charged spherical particles in the bulk is well known to be described by a Yukawa potential [20, 21]

$$\beta U(r) = \beta u_{pair}(r) = (Z^*)^2 \lambda_B \left( \frac{e^{\kappa R}}{1 + \kappa R} \right)^2 \frac{e^{-\kappa r}}{r}, \quad (4)$$

where  $Z^*$  is the renormalized charge [22] of the particles,  $\lambda_B$  the Bjerrum-length characterizing the solvent ( $\lambda_B = e^2/4\pi\epsilon\epsilon_0 k_B T$ , with  $\epsilon$  the dielectric constant of the solvent and  $e$  the elementary charge),  $\kappa^{-1}$  the Debye screening length (given by the salt concentration in the solution),  $R$  the particle radius and  $r$  the centre-centre distance of the particles. Fig.3 shows the experimentally determined pair-potential (symbols) together with a fit to Eq.(4) (solid line). As can be seen, our data are well described by Eq.(4). As fitting parameters we obtained  $Z^* \approx 6500$  electron charges and  $\kappa^{-1} \approx 470\text{nm}$ , respectively. The renormalized charge is in good agreement with the predicted value of the saturated effective charge of our particles [23, 24] and the screening length agrees reasonably with the bulk salt concentration in our suspension as obtained from the ionic conductivity. Given the additional presence of a charged substrate, it might seem surprising that Eq.(4) describes our data successfully. However, it has been demonstrated experimentally [25] and theoretically [26, 27] that a Yukawa-potential captures the leading order interaction also for colloids close to a charged wall. A confining wall introduces only a very weak (below  $0.1 k_B T$ ) correction due to additional dipole repulsion. This correction is below our experimental resolution. Repeating the two-body measurements with different laser intensities (50mW to 600mW) yielded within our experimental resolution identical pair potential parameters. This also demonstrates that possible light-induced particle interactions (e.g. optical binding [28]) are negligible. The approach of the third and fourth particle by means of an additional optical trap could, in principle, lead to additional light-induced interactions between the laser spot and the two particles kept in the line trap. To exclude such effects, we repeated the two-particle measurements and approached an empty trap (without the third particle) to the line trap where the two particles were fluctuating. Within our experimental resolution, we again observed identical pair potentials, which suggests, that the additional optical trap has no influence on the two particles in the line trap. When the third or fourth particle are present at a distance  $d$  along the perpendicular bisector of the scanned laser line (cf.

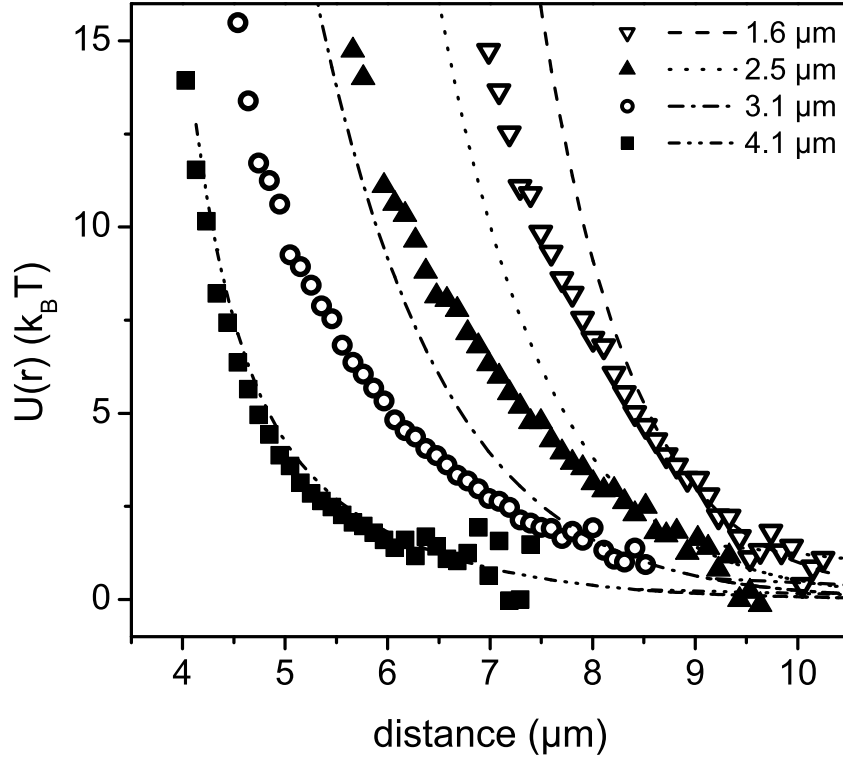


FIG. 4: Experimentally determined interaction energy  $U(r)$  (symbols) for two particles in a line tweezers in the presence of a fixed third particle with distance  $d$  on the perpendicular bisector of the line trap. For comparison the superposition of three pair-potentials is plotted as lines. Symbols and lines are labelled by the value of  $d$ .

inset of Fig.1), the total interaction energy  $U(r, d)$  is not simply given by the sum of the pair-interaction potentials Eq.(4) alone but also contains additional many-body terms. Following the definition of McMillan and Mayer [29],  $U(r, d)$  is given by

$$U(r, d) = \sum_{i \neq j} u_{pair}(r_{ij}) + u_{many-body} , \quad (5)$$

with  $u_{pair}(r_{ij})$  being the pair-potential between particles  $i$  and  $j$  as defined in Eq.(4), indices  $i$  and  $j$  run from 1 to the number of particles. The last term,  $u_{many-body}$  is the sum of many-body interaction potentials. In the case of three particles  $u_{many-body} \equiv u_{123}(r_{12}, r_{13}, r_{23})$  and Eq.(5) reduces to

$$U(r, d) = u_{pair}(r_{12}) + u_{pair}(r_{13}) + u_{pair}(r_{23}) + u_{123}(r_{12}, r_{13}, r_{23}) . \quad (6)$$

Distances  $r_{ij}$  are the distances between the three particles in the system which can, due to the chosen symmetric configuration ( $r_{23} \equiv r_{13}$ ), be expressed by the two variables  $r = r_{12}$  and  $d = \sqrt{r_{13}^2 - (r/2)^2}$ . We have followed the same procedure as described above for the case of two particles. First, we have measured the probability distribution  $P(r; d)$  of the two particles in the laser trap with the third particle fixed at distance  $d$  from the trap. Taking the logarithm of  $P(r; d)$  we extracted the total interaction energy  $U(r, d)$ . When approaching the third particle, the two particles in the trap are slightly displaced in the  $y$ -direction at small  $r$ . Accordingly, the minimum energy configurations of the two particles are not on a straight line as before. The most likely configuration at given distance  $r$  is  $(x_1 = r/2, y_1 = y(r), x_2 = -r/2, y_2 = y(r))$  with  $y(r)$  given by the measured particle positions. Since we have the full knowledge of the two-dimensional external laser potential, we can compute  $u_L(r/2, y(r))$  for every given

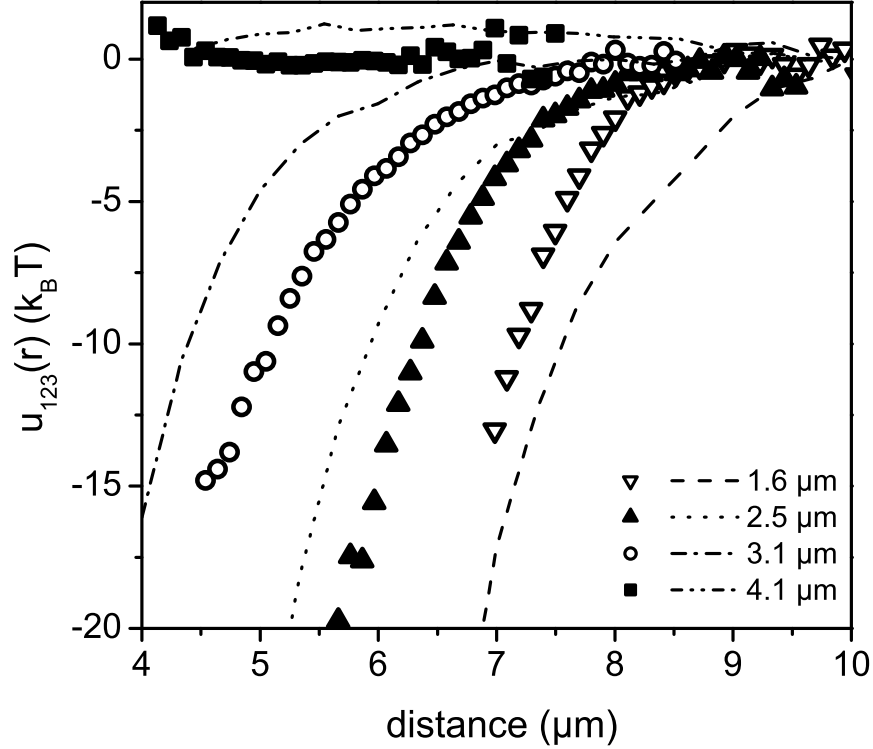


FIG. 5: Three-body potentials for different  $d$ . Measured three-body potentials indicated by symbols. The lines are three-body potentials as obtained from the solutions of the nonlinear Poisson-Boltzmann equation for three colloids arranged as in the experiment. The parameters in the Poisson-Boltzmann calculation were chosen so that the pair-interaction potentials were correctly reproduced. Symbols and lines are labeled by the value of  $d$ .

configuration and use it in the Eq.(2) instead of  $u_L(r/2, 0)$ . The results are plotted as symbols in Fig.4 for the distance of the third particle  $d = 4.1, 3.1, 2.5$  and  $1.6 \mu\text{m}$ , respectively. As expected,  $U(r, d)$  becomes larger as  $d$  decreases due to the additional repulsion between the two particles in the trap and the third particle. In order to test whether the interaction potential can be understood in terms of a pure superposition of pair-interactions, we first calculated  $U(r, d)$  according to Eq.(6) with  $u_{123} \equiv 0$ . This was easily achieved because the positions of all three particles were determined during the experiment and the distance-dependent pair-potential is known from the two-particle measurement described above (Fig.3). The results are plotted as dashed lines in Fig.4. Considerable deviations from the experimental data can be observed, in particular at smaller  $d$ . These deviations can only be explained, if we take three-body interactions into account. Obviously, at the largest distance, i.e.  $d = 4.1 \mu\text{m}$  our data are well described by a sum over pair-potentials which is not surprising, since the third particle cannot influence the interaction between the other two, if it is far away from both. In agreement with theoretical predictions [31], the three-body interactions therefore decrease with increasing distance  $d$ .

According to Eq.(6) the three-body interaction potential (the only many-body term in case of only three particles) is simply given by the difference between the measured  $U(r, d)$  and the sum of the pair-potentials (i.e. by the difference between the measured data and their corresponding lines in Fig.4). The results are plotted as symbols in Fig.5. It is clearly seen, that in the case of charged colloids  $u_{123}$  is entirely attractive and becomes stronger as the third particle approaches. It is also interesting to see that the range of  $u_{123}$  is of the same order as the pair-interaction potentials. It might seem surprising that it is possible to sample the potential up to energies of  $15k_B T$ , as configurations of such a high energy statistically happen only with very low probability. In this experiment we can choose the energetic range of the potential we want to sample by adjusting the strength of the line tweezers. The laser potential pushes the particles together, which allows us to sample different ranges of the electrostatic potential. Thus, to achieve a

better resolution for smaller particle separations (e.g. higher potential values), the strength of the line tweezers had to be increased. The shape of the external potential  $u_L$  was independent of the strength of the laser beam (see Fig.2) and the magnitude scaled linearly with the input laser power. This allowed us to adjust the input laser intensity so as to obtain a suitable particle separation range. The external potential was obtained simply by scaling the Gaussian shown in Fig.2.

#### IV. FOUR-BODY INTERACTIONS

The fourth particle has been placed symmetrically to the third one at the distance  $d$  from the line trap by means of an additional focussed laser tweezers. Like the third particle it was kept fixed at this position during the experiment. The data evaluation is identical to the evaluation in the case of three particles, the distance probability  $P(r)$  of the two particles in the line trap is analysed, from which the total interaction potential is obtained. After subtracting the pair energies we have obtained the total many-body interaction potential  $u_{\text{many-body}}$ . In the case of three particles the total many-body interaction potential was simply the three-body term  $u_{123}$ , but with four particles it consists of more terms. In the experiment the interaction between the two colloids in the line trap was observed. When the third particle was introduced, the interaction was altered and the amount to which it has changed was called the three-body interaction potential. Now, as we add another particle, we expect to see the same three-body effect once again, i.e. the total change of interaction should be twice the three-body term. This would be true if there were no four-body interactions, but with the four-body term the total many-body interaction potential is  $u_{\text{many-body}} = 2u_{123}(r, d) + u_{1234}(r, d)$ . The four-body interaction potential can thus be extracted,

$$u_{1234}(r, d) = U(r, d) - \sum_{i \neq j} u_{\text{pair}}(r_{ij}) - 2u_{123}(r, d) . \quad (7)$$

The four-body potential  $u_{1234}(r, d)$  depends only on the two parameters  $(r, d)$  due to the chosen symmetric configuration. The pair and three-body terms are obtained from the previous measurements. The results are presented on Fig.6. The solid lines represent the many-body interaction energies obtained from the four-body experiments. The dashed lines are the three-body interaction energies obtained from the three-body experiments at the same conditions. There are three pairs of curves on the figure. Each pair corresponds to a certain distance  $d$  of the third and fourth particle from the line trap. From the upper to the lower pair the distances were  $d = 4.2\mu\text{m}, 3.0\mu\text{m}, 2.4\mu\text{m}$ . Again, when the third and fourth particles were very far from the line trap ( $d = 4.2\mu\text{m}$ ), the many-body term vanishes. When they are placed closer, there is an attractive three-body interaction already discussed (dashed lines,  $d = 3.0\mu\text{m}, 2.4\mu\text{m}$ ). Also the total many-body interaction in the four-body experiment (solid lines,  $d = 3.0\mu\text{m}, 2.4\mu\text{m}$ ) is attractive and, curiously, quite similar to the three-body term. Applying Eq.7 we can conclude that the four-body interaction is repulsive and of about the same range and magnitude as the attractive three-body term,

$$u_{1234}(r, d) \approx -u_{123}(r, d) . \quad (8)$$

The curiosity appearing in the two configurations explored, is that the total many-body interaction potential lies almost on top of the three-body term. If this was a universal conclusion, it would mean that the three-body terms are partially canceled by the four-body interaction potentials, i.e., we could include the four-body interaction simply by counting only half of the three-body terms. However, while this would certainly be an interesting feature, we must be aware of the fact that only two single configurations were studied here, not enabling us to draw very general conclusions.

#### V. NUMERICAL CALCULATIONS

In order to get more information about three-body potentials in colloidal systems, we additionally performed non-linear Poisson-Boltzmann (PB) calculations [30], in a similar way as in [31]. The PB theory provides a mean-field description in which the micro-ions in the solvent are treated within a continuum approach, neglecting correlation effects between the micro-ions. It has repeatedly been demonstrated [32, 33] that in case of monovalent micro-ions the PB theory provides a reliable description of colloidal interactions. The interactions among colloids are, on this level, mediated by the continuous distribution of the microions and can be obtained once the local electrostatic potential due to the microionic distribution is known. The normalized electrostatic potential  $\psi(x, y, z)$ , which is the solution

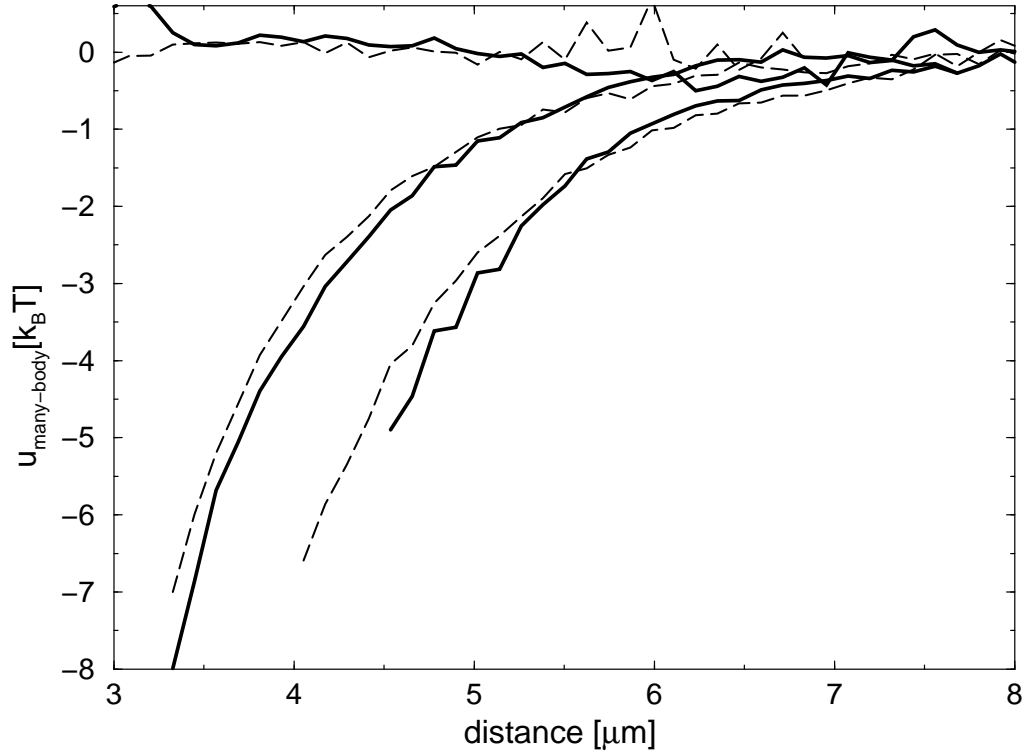


FIG. 6: Experimentally determined total many-body potential (three- and four-body terms superposed) in the configuration of four particles (solid lines) plotted together with the three-body potential in the three particle case (dashed lines). The three sets of curves correspond to different distances  $d$  of the third and the fourth particle from the baseline. From below they correspond to  $d = 2.4\mu m$ ,  $d = 3.0\mu m$  and  $d = 4.2\mu m$ . In the latter case the third and fourth particles are so far away, that the measured many-body interaction vanishes. In the other two cases the four-body interaction term is opposite and of the same size as the three-body term, so that the total many-body interaction potential, which is  $u_{\text{many-body}} = 2u_{123} + u_{1224}$ , looks almost as the three-body term. See also the text in the section *Four-body interactions*. The three-body interaction potential here differs from the one on Fig.5, while the experimental conditions (salt concentration) were slightly different in this set of measurements.

of the non-linear PB equation,

$$\begin{aligned} \nabla^2 \psi(\vec{r}) &= \kappa^2 \sinh \psi(\vec{r}) , \\ \mathbf{n} \cdot \nabla \psi &= 4\pi\lambda_B \sigma , \quad \vec{r} \text{ on colloid surface} , \end{aligned} \quad (9)$$

describes the equilibrium distribution of the microions around a given macroionic configuration. Here  $\kappa$  is the inverse Debye screening length,  $\lambda_B$  the Bjerrum length ( $\lambda_B = 0.72\text{nm}$  for aqueous solutions at room temperature) and  $\sigma$  is the surface charge density on the colloid surface (constant charge boundaries are assumed for all colloids in the system).  $\mathbf{n}$  is the normal unit vector on the colloid surface. We used the multi-centered technique, described and tested in other studies [2, 3, 4, 30] to solve the PB equation (9) at fixed configurations of three colloids and obtain the electrostatic potential  $\psi(x, y, z)$ , which is related to the micro ionic charge density. Integrating the stress tensor, depending on  $\psi(x, y, z)$ , over a surface enclosing one particle, results in the force acting on this particle. First, we calculated how the force  $f_{12}$ , and from it the pair-potential between two particles, depend on the distance between isolated two particles. Choosing the suitable bare charge on the colloid surface, we were able to reproduce the measured pair-interaction in Fig.3. The calculation of three-body potentials was then carried out by calculating the total force acting on one particle in the line trap (say, particle 1) in the presence of all three particles and subtracting the corresponding pair-forces  $f_{12}$  and  $f_{13}$  obtained previously in the two-particle calculation. If there is any difference between the force on particle 1 obtained from the full PB solution for the three particle configuration and the sum of two two-body forces, this difference is due to the three-body interactions in the system. The difference is then integrated to obtain the three-body potential. The results are plotted as dashed and dotted lines in Fig.5 and show qualitative agreement with the experimental data. To account for the deviations from the experimental data one has to take into account the following points: **(i)** there is a limited experimental accuracy to which the light potential can be determined. The accuracy decreases with increasing laser intensity (note that normalized potentials are plotted

in Fig.2). In the three-body experiments, due to the presence of the third repulsive particle, a stronger light field is needed and the experimental error in determining the light potential is estimated to be around  $\pm 1k_B T$ . Since we have to subtract the light potential twice from the total potential to obtain the three-body potential, this error doubles and we expect an error of about  $\pm 2k_B T$  in the final result. **(ii)** An error of about  $\pm 2k_B T$  should be expected in the numerically obtained three-body potentials as well. **(iii)** While in the numerical calculation we assume identical colloidal spheres, in the experiment small differences with respect to the size and the surface charge are unavoidable. This effect, however, is rather small and leads to deviations on the order of 5 percent of the total potential. **(iv)** The numerical calculations do not take into account any effects which may be caused by the substrate. Although we expect such effects to be rather small (similar to the contribution for the pair potential) they can not completely ruled out. Considering the above mentioned uncertainties it should be emphasized that in particular the sign and the order of magnitude of the calculated potential compares well with our measured results. This strongly supports our interpretation of the experimental results in terms of the three-body interactions.

Having solved the Poisson-Boltzmann equation we have the complete knowledge of the electrostatic potential in the space around the colloids and can therefore observe the microscopic effects leading to the many-body interactions [3]. The many-body interactions are a consequence of the nonlinearity of the physical equations governing the interactions in our system. Due to the nonlinearity the electrolyte density is different than a description based on the pairwise additivity would predict. We have observed that there are less counterions in the region among the colloids than one would expect when superposing pair potentials. Less counterions means less screening and larger electrostatic energy, but also larger entropy and at the end, obviously, smaller free energy. One could conclude, that on the microscopic electrolyte level the many-body interactions are entropy-driven.

## VI. CONCLUSIONS

We have demonstrated that the three-body interactions among charged colloids in suspension are attractive and of the same range as the pair-interactions. They present a considerable contribution to the total interaction energy and have to be taken into account. Further, for a limited number of configurations, also the four-body interactions have been explored. They have been found to be repulsive and of similar range and magnitude as three-body and pair terms. For the two configurations studied, the four-body interaction is almost precisely the opposite of the three-body interaction in the system of three particles. Thus, adding the fourth particle and the four-body interaction term simply cancels one of the two three-body terms and the total many-body interaction potential  $u_{\text{many-body}} = 2u_{123} + u_{1234}$  is equal to the three-body term  $u_{123}$  [17, 18]. The total many-body contribution stays attractive, although the four body interaction alone is repulsive.

Whenever dealing with systems comprised of many particles, in principle also higher-order terms have to be considered. The relative weight of such higher-order terms depends on the particle number density  $\rho$ . While at low enough  $\rho$  a pure pair-wise description should be sufficient, with increasing density first three-body, four-body interactions and then higher-order terms come into play. One could speculate that there is an intermediate density regime, where the macroscopic properties of systems can be successfully described by taking into account only two- and three-body interactions [34] and, going up with the density, also the regime where two-, three- and four-body terms are sufficient. Indeed liquid rare gases [9] and the island distribution of adsorbates on crystalline surfaces [14] are examples where the thermodynamic properties are correctly captured by a description limited to pair- and three-body (AT-triple dipole interactions, either attractive or repulsive, depending on the configuration of the particles) interactions.

However, it is difficult to predict in which range of parameters such an assumption is justified. Especially the fact observed in this work, that the four-body term compare with the three-body term in magnitude, should render such an approach questionable. If one, describing a suspension, only takes two- and three-body effects into account, one takes too much attraction on board. We have seen in two examples in this paper, that the repulsive four-body interactions significantly reduce the attractive three-body interaction. Theoretical models taking two- and three-body effects into account [34] are therefore of very limited value in describing a dense system. The continuation in this direction (five-, six- body, ...interactions) does not seem promising, especially since the series even does not seem to converge and other methods have to be applied to capture the many-body effects. In the colloidal suspension all many-body interaction potentials are correctly taken into account by performing the non-linear Poisson-Boltzmann calculations. This has been done in [2, 3, 4] where solid-liquid phase behaviour was investigated by Poisson-Boltzmann Brownian dynamics simulations. The conclusion there was that the total many-body interaction does not vanish, but is attractive and

leads to notable macroscopic effects, e.g. to a shift of the melting line in colloidal suspensions.

- 
- [1] A. A. Louis, *J. Phys.: Condens. Matter* 14 (40), 9187 (2002).
  - [2] J. Dobnikar, R. Rzehak, and H. H. von Grünberg, *Europhys. Lett.* 61, 695 (2003).
  - [3] J. Dobnikar, Y. Chen, R. Rzehak, and H. H. von Grünberg, *J. Chem. Phys.* 119 (9) (2003).
  - [4] J. Dobnikar, Y. Chen, R. Rzehak, and H. H. von Grünberg, *J. Phys. Condens. Matter* 15(1) S263-S268 (2003).
  - [5] M. Brunner, C. Bechinger, W. Strepp, V. Lobaskin, and H. H. von Grünberg, *Europhys. Lett.* 58, 926 (2002).
  - [6] B. M. Axilrod and E. Teller, *J. Chem. Phys.* 11, 299 (1943).
  - [7] J. A. Barker, D. Henderson, *Rev. Mod. Phys.* 48, 587 (1976).
  - [8] J. M. Bomont and J. L. Bretonnet, *Phys. Rev. B* 65, 224203 (2002).
  - [9] N. Jakse, J. M. Bomont, and J. L. Bretonnet, *J. Chem. Phys.* 116, 8504 (2002).
  - [10] F. Formisano, C. J. Benmore, U. Bafle, F. Barocchi, P. A. Egelstaff, R. Magli, and P. Verkerk, *Phys. Rev. Lett.* 79, 221 (1997).
  - [11] F. Formisano, F. Barocchi, and R. Magli, *Phys. Rev. E* 58, 2648 (1998).
  - [12] J. W. Negele, *Nucl. Phys. A* 669, 18 (2002).
  - [13] J. Hafner, *From Hamiltonians to phase diagrams* (Springer, Berlin, Heidelberg, 1987).
  - [14] L. Österlund, M. O. Pedersen, I. Stensgaard, E. Laegsgaard, and F. Besenbacher, *Phys. Rev. Lett.* 83, 4812 (1999).
  - [15] M. Ovchinnikov and V. A. Apkarian, *J. Chem. Phys.* 110, 9842 (1999).
  - [16] K. Binder and D. P. Landau, *Surf. Sci.* 108, 503 (1981).
  - [17] M. Brunner, J. Dobnikar, H. H. von Grünberg and C. Bechinger, *Phys. Rev. Lett.* 92, 78301 (2004).
  - [18] J. Dobnikar, M. Brunner, H. H. von Grünberg and C. Bechinger, *Phys. Rev. E*, 69, 31402 (2004).
  - [19] T. Palberg, W. Härtl, U. Wittig, H. Versmold, M. Würth, and E. Simmacher, *J. Phys. Chem.* 96, 8180 (1992).
  - [20] B. V. Derjaguin and L. Landau, *Acta Physicochim U.R.S.S.* 14, 633 (1941).
  - [21] E. J. W. Vervey and J. T. G. Overbeek, *Theory of the stability of lyophobic colloids* (Elsevier, Amsterdam, 1948).
  - [22] L. Belloni, *J. Phys. Cond. Mat.* 12, R549 (2000).
  - [23] The saturated effective charge of our particles is about 6900 for water at room temperature.
  - [24] E. Trizac, *J. Phys. A: Math. Gen.* 36, 5835 (2003).
  - [25] S. H. Behrens and D. G. Grier, *Phys. Rev. E* 64, 50401 (2001).
  - [26] F. H. Stillinger, *J. Chem. Phys.* 35, 1584 (1961).
  - [27] R. R. Netz and H. Orland, *Eur. Phys. J. E.* 1, 203 (2000).
  - [28] M. M. Burns, J. M. Fournier, and J. A. Golovchenko, *Phys. Rev. Lett.* 63, 1233 (1989).
  - [29] W. McMillan and J. Mayer, *J. Chem. Phys.* 13, 276 (1945).
  - [30] J. Dobnikar, D. Haložan, M. Brumen, H. H. von Grünberg and R. Rzehak, *Comp. Phys. Comm.*, 159/2, 73-92 (2004).
  - [31] C. Russ, R. van Roij, M. Dijkstra, and H. H. von Grünberg, *Phys. Rev. E* 66, 011402 (2002). *Europhys. Lett.* 58, 926 (2002).
  - [32] R. D. Groot, *J. Chem. Phys.* 95, 9191 (1991).
  - [33] Y. Levin, *Rep. Prog. Phys.* 65, 1577 (2002).
  - [34] A.-P. Hynninen, M. Dijkstra and R. van Roij, *J. Phys. Cond. Mat.* 15 (48), S3549 (2003).